Free Boundary Conditions Active Contours with Applications for Vision

Supplementary Material

Michal Shemesh and Ohad Ben-Shahar
shemeshm,ben-shahar@cs.bgu.ac.il

Ben-Gurion University of the Negev, Beer-Sheva, Israel

1 The variational problem for $y = y(x)$

Assume one represents the OAC as a function, i.e., as $y = y(x)$, where one coordinate is a function of the other. This choice is particularly attractive if we intentionally want to force a strictly monotonic behavior at the representational level of the OAC. For simplicity, suppose further that the energy functional over the curve is limited to first order derivatives. Under these assumptions the energy functional

$$\begin{aligned} E_{curve} &= \int_0^1 \left[\alpha |y'(x)|^2 + g(x)\right] dx \\ g(x) &= -\gamma \left|\nabla (G_\sigma * I(y(x)))\right| \ , \end{aligned} \tag{1}$$

can be written generally as

$$J[y] = \int_{x_0}^{x_1} F(x, y, y') dx \ , \tag{2}$$

and our goal is to find those curves $y = y(x)$ for which this functional obtains a minimum. Following calculus of variation [1, pp. 54-61], the necessary condition on $y(x)$ such the $J[y]$ is minimized is that it solves the corresponding Euler Lagrange equation, i.e.,

$$F_y - \frac{d}{dx} F_{y'} = 0 \ . \tag{3}$$

Suppose now that the two end points of the active contour, i.e, $P_0 \stackrel{\triangle}{=} y(x_0)$ and $P_1 \stackrel{\triangle}{=} y(x_1)$ are constrained to lie on two smooth boundary curves defined as functions $B_0(x)$ and $B_1(x)$, respectively. Hence

$$\begin{aligned} P_0 &= y(x_0) = B_0(x_0) \\ P_1 &= y(x_1) = B_1(x_1) \ , \end{aligned} \tag{4}$$

where x_0 and x_1 are unknowns, as illustrated in Fig. 1a. According to these free

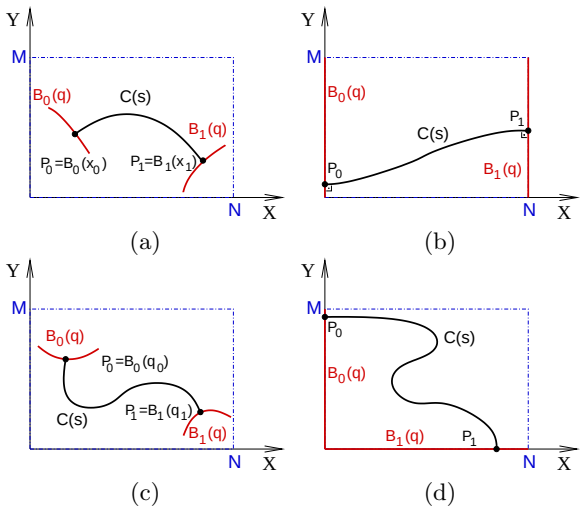

Fig. 1. The basic elements of OACs with free boundary conditions, where each end point is restricted to lie on a different boundary curve. Four typical examples for such OAC (shown in black) and boundary curves (shown in red) drawn on an image $I : [0, M] \times [0, N]$. **(a):** An OAC which is represented as a function of one variable, i.e. $C(s) = (s, y(s))$, where the boundary curves are two functions $B_0(q)$ and $B_1(q)$. **(b):** An OAC of the same type as in panel a, where the boundary curves are two vertical lines $B_0(q) = (0, q)$ and $B_1(q) = (M, q)$ which coincide with opposite image margins. **(c):** An OAC which is represented as a parametric curve $C(s) = (x(s), y(s))$. In this general case the boundary curves can be arbitrary plane parametric curves. **(d):** An OAC of the same type as in panel c, where the boundary curves are two straight lines $B_0(q) = (0, q)$ and $B_1(q) = (q, 0)$, which coincide with two boundaries of image I.

boundary conditions, it is also necessary to satisfy certain boundary constraints at the end points

$$\begin{aligned} [F + (B_0' - y')F_{y'}]|_{x=x_0} &= 0 \\ [F + (B_1' - y')F_{y'}]|_{x=x_1} &= 0 \ . \end{aligned} \tag{5}$$

In case the boundary curves are two straight lines parallel to the y-axis [1, pp. 25-26], i.e. $B_0 = (x_0, y)$ and $B_1 = (x_1, y)$ as illustrated in Fig. 1b, a necessary condition for a curve $y(x)$ to be a minimum point of $J[y]$, is a vanishing first variation of the functional, i.e.,

$$\delta J = \int_{x_0}^{x_1} F_y h + F_{y'} h' dx = 0 \ . \tag{6}$$

Using integration by parts of the second term further yields

$$\delta J = \int_{x_0}^{x_1} (F_y - \frac{d}{dx} F_{y'}) h dx + F_{y'} h|_{x=x_0}^{x=x_1} = 0 \ . \tag{7}$$

where $h = h(x)$ is an arbitrary "increment" of the "dependent variable" $y = y(x)$. If we consider functions h where $h(x_0) = h(x_1) = 0$ (as would be the case for *fixed* boundary conditions), the last terms in Eq. 7 vanishes and the condition $\delta J[y] = 0$ implies

$$F_y - \frac{d}{dx} F_{y'} = 0 \,, \tag{8}$$

i.e., y is the solution of the corresponding Euler-Lagrange equation. Clearly, for free boundary conditions active contours, $h(x_0)$, $h(x_1)$ do not necessarily vanish and since their value might be arbitrary, the only way the last terms of Eq. 7 could also vanish is by the constraints

$$\begin{aligned} F_{y'}|_{x=x_0} &= 0 \\ F_{y'}|_{x=x_1} &= 0 \ . \end{aligned} \tag{9}$$

Under this assumption of vertical boundary curves, let us assume now that the energy functional from Eq. 1 includes second order derivatives, meaning

$$J[y] = \int_{x_0}^{x_1} F(x, y, y', y'') dx \,. \tag{10}$$

Following calculus of variation again, a necessary condition for a curve $y(x)$ to be a minimum point of $J[y]$, is a vanishing first variation of the functional, i.e.,

$$\begin{aligned} \delta J = \textstyle\int_{x_0}^{x_1} [F_y - \frac{d}{dx} F_{y'} + \frac{d^2}{dx^2} F_{y''}] h dx + \\ h[F_{y'} - \frac{d}{dx} F_{y''}]\big|_{x=0}^{x=1} + [h' F_{y''}]|_{x=x_0}^{x=x_1} = 0 \,. \end{aligned} \tag{11}$$

As mentioned above, if we consider functions h where $h(x_0) = h(x_1) = 0$ and $h'(x_0) = h'(x_1) = 0$ the last terms in Eq. 11 vanishes and the condition $\delta J[y] = 0$ implies

$$F_y - \frac{d}{dx} F_{y'} + \frac{d^2}{dx^2} F_{y''} = 0 \,, \tag{12}$$

i.e., y is the solution of the corresponding Euler-Lagrange equation. Since $h(x_0)$, $h(x_1)$, $h'(x_0)$ and $h'(x_1)$ do not necessarily vanish and since their value might be arbitrary, the only way the last terms of Eq. 11 could also vanish is by the constraint

$$\begin{aligned} [F_{y'} - \tfrac{d}{dx} F_{y''}]\big|_{x=x_0} = 0 \qquad F_{y''}|_{x=x_0} = 0 \\ [F_{y'} - \tfrac{d}{dx} F_{y''}]\big|_{x=x_1} = 0 \qquad F_{y''}|_{x=x_1} = 0 \ . \end{aligned} \tag{13}$$

1.1 Implementation

Consider the case where the energy functional over the curve is limited to first order derivatives (Eq.3), and the energy functional is defined as in Eq. 1. Applying Eq. 3 yields the following Euler-Lagrange equation

$$F_y - \frac{d}{dx} F_{y'} = 0 \quad \Rightarrow \quad -2\alpha y'' + \frac{\partial}{\partial y} g = 0 \ . \tag{14}$$

Under the assumption of vertical boundary curves, the end point constraint from Eq. 9 becomes

$$\begin{aligned} F_{y'}|_{x=x_0} &= 2\alpha y'|_{x=x_0} = 0 \quad \Rightarrow \quad y'|_{x=x_0} = 0 \\ F_{y'}|_{x=x_1} &= 2\alpha y'|_{x=x_1} = 0 \quad \Rightarrow \quad y'|_{x=x_1} = 0 \ . \end{aligned} \tag{15}$$

For horizontal boundary curves the derivation is analogous.

In the case where the functional include second derivatives (see Eq. 10), and the energy functional is defined as

$$\begin{aligned} E_{curve} &= \int_0^1 \left[\alpha|y'(x)|^2 + \beta|y''(x)|^2 + g(x)\right] dx \\ g(x) &= -\gamma \left|\nabla(G_\sigma * I(y(x)))\right| \ , \end{aligned} \tag{16}$$

Applying Eq. 12 yields the following Euler-Lagrange equation

$$\begin{aligned} F_y - \tfrac{d}{dx}F_{y'} + \tfrac{d^2}{dx^2}F_{y''} = 0 \quad \Rightarrow \\ -2\alpha y'' + 2\beta y'''' + \tfrac{\partial}{\partial y} g = 0 \ . \end{aligned} \tag{17}$$

Under the assumption of vertical boundary curves, the end point constraint from Eq. 13 becomes

$$\begin{aligned} &[F_{y'} - \tfrac{d}{dx}F_{y''}]\big|_{x=x_0,x_1} = 0 \\ &F_{y''}|_{x=x_0,x_1} = 0 \end{aligned} \quad \Rightarrow$$

$$\begin{aligned} &[2\alpha y' - 2\beta y''']\big|_{x=x_0,x_1} = 0 \\ &2\beta y''|_{x=x_0,x_1} = 0 \end{aligned} \quad \Rightarrow \tag{18}$$

$$\begin{aligned} &[y' = y''']\big|_{x=x_0,x_1} = 0 \\ &y''|_{x=x_0,x_1} = 0 \ . \end{aligned}$$

For horizontal boundary curves the derivation is analogous.

2 Numerical considerations for a typical visual OAC

As mentioned in the paper, the time evolution of the OAC, now represented as a parametric curve $C(s) = (x(s), y(s))$, toward its optimal energetic configuration is guided by the steepest descent equation

$$C_t(s,t) \triangleq \frac{\partial}{\partial t} C(s,t) = -2\alpha C''(s,t) + \nabla g(s,t) \ . \tag{19}$$

Indeed, starting from an initial curve $C(s,0)$, this process converges to a stationary state when $\frac{\partial}{\partial t}C(s,t)$ vanishes, i.e., when the curve satisfies the necessary condition

$$\begin{aligned} \Phi_x - \tfrac{d}{ds}\Phi_{x'} = 0 \quad \Rightarrow \quad -2\alpha x'' + \tfrac{\partial}{\partial x} g = 0 \\ \Phi_x - \tfrac{d}{ds}\Phi_{y'} = 0 \quad \Rightarrow \quad -2\alpha y'' + \tfrac{\partial}{\partial y} g = 0 \ . \end{aligned} \tag{20}$$

In practice, the OAC is represented as a time-evolving series of *control points* $\{x_i^t, y_i^t\}$ for $i = 1...n$ and therefore all derivatives are computed numerically using central differences. For the OAC's internal points we use second order central differences with $O(h^2)$ approximation error

$$x_i'' = \frac{2}{h_{i-1}(h_{i-1}+h_i)}x_{i-1} + \frac{-2}{h_{i-1}h_i}x_i + \frac{2}{h_i(h_{i-1}+h_i)}x_{i+1} \ , \tag{21}$$

where $h_i = |x_{i+1} - x_i|$.

Unlike in common active contours which are closed, however, this approximation does not apply to end points. To compute the derivatives of these end points, we use second order forward and backward differences formulas. In particular, the backward differences approximation for the last two points of the seam is given by

$$\begin{aligned} x_i'' = &(\tfrac{2(h_{i-3}+2h_{i-2}+3h_{i-1})}{(h_{i-3}+h_{i-2}+h_{i-1})(h_{i-2}+h_{i-1})(h_{i-1})})x_i - \\ &(\tfrac{2(h_{i-3}+2h_{i-2}+2h_{i-1})}{(h_{i-3}+h_{i-2})(h_{i-2})(h_{i-1})})x_{i-1} + \\ &(\tfrac{2(h_{i-3}+h_{i-2}+2h_{i-1})}{(h_{i-3})(h_{i-2})(h_{i-2}+h_{i-1})})x_{i-2} - \\ &(\tfrac{2(h_{i-2}+2h_{i-1})}{(h_{i-3})(h_{i-3}+h_{i-2})(h_{i-3}+h_{i-2}+h_{i-1})})x_{i-3} \ , \end{aligned} \tag{22}$$

The forward differences formula for the first two points is completely analogous.

Since all these numerical approximations are linear combinations of curve points, the convergence conditions from Eq. 20 can be written as a pair of matrix linear equations

$$\begin{aligned} A\,x(s,t) + \tfrac{\partial}{\partial x}g = 0 \\ A\,y(s,t) + \tfrac{\partial}{\partial y}g = 0 \ . \end{aligned} \tag{23}$$

where $x = (x_1, ..., x_n)$ and $y = (y_1, ..., y_n)$ are the coordinate vectors of all control points and the A matrix incorporates the weighting of the numerical approximations. As is done in numerous active contour studies [2–7], the solution of Eq. 23, and the time evolution of the OAC, is done via Euler's method using the following algebraic formulas

$$\begin{aligned} x^{t+1} = (A + \delta I_n)^{-1}(\delta x^t + \tfrac{\partial}{\partial x}g(x^t, y^t)) \\ y^{t+1} = (A + \delta I_n)^{-1}(\delta y^t + \tfrac{\partial}{\partial y}g(x^t, y^t)) \end{aligned} \tag{24}$$

where δ is the step size and I_n is the unit matrix of size $n \times n$.

The set of coordinates obtained from Eq. 24 provides the next time step in the OAC's evolution, without taking into account the free boundary conditions.

To do so in a way that respects transversality constraints

$$\begin{aligned}
&(\Phi_{x'}, \Phi_{y'})|_{s=0} \cdot (X_0', Y_0')|_{q_0} = 0 \\
&(\Phi_{x'}, \Phi_{y'})|_{s=1} \cdot (X_1', Y_1')|_{q_1} = 0 \\
&\Rightarrow \\
&2\alpha\ (x', y')|_{s=0} \cdot (X_0', Y_0')|_{q_0} = 0 \\
&2\alpha\ (x', y')|_{s=1} \cdot (X_1', Y_1')|_{q_1} = 0\ ,
\end{aligned} \tag{25}$$

one must adjust the end points (points 1 and n) such that they remain on the boundary curves and also satisfy the transversality constraint, i.e., placed on the boundary curves such that the boundary curves are perpendicular to the OAC.

Finally, we mention that the time evolution of the OAC may shift control points significantly over time, and create non uniform sampling density along its length. Although not necessary for the correctness of the computations, re-sampling of the curve for equally dense control points after each iteration provides not only better numerical stability, but also better control over the the curve for further use in different applications.

References

1. Gelfand, I., Fomin, S.: Calculus of Variations. Prentice-Hall, Inc. (1963)
2. Kass, M., Witkin, A., Trezopoulos: Snakes: Active contour models. Int. J. Comput. Vision **1** (1988) 321–331
3. Berger, M.O., Mohr, R.: Towards autonomy in active contour models. In: ICPR. Volume 1. (1990) 847–851
4. Amini, A., Tehrani, S., Weymouth, T.: Using dynamic programming for minimizing the energy of active contours in the presence of hard constraints. In: ICCV. (1988) 95–99
5. Waite, J.B., Welsh, W.J.: An application of active contour models to head boundary location. In: British Machine Vision Conference. (1990) 407–412
6. Cohen, L.D.: On active contour models and balloons. CVGIP **53** (1991) 221–218
7. Li, H., Shen, T., Smith, M.B., Fujiwara, I., Vavylonis, D., Huang, X.: Automated actin filament segmentation, tracking and tip elongation measurements based on open active contour models. IEEE Int. Symp. on Biomed. Imaging **15** (2009)
8. Baldonado, M., Chang, C.C., Gravano, L., Paepcke, A.: The stanford digital library metadata architecture. Int. J. Digit. Libr. **1** (1997) 108–121